Progress In Electromagnetics Research Letters, Vol. 95, 147–153, 2021

Dual-Band Bandpass Filter Design Using Stub-Loaded Hairpin Resonator and Meandering Uniform Impedance Resonator

Yun Xiu Wang*, Yuan Li Chen, Wen Hui Zou, Wei Chao Yang, and Jin Zen

Abstract—A novel microstrip dual-band bandpass filter (BPF) by coupling a stub-loaded hairpin resonator and two stub-loaded uniform impedance resonators (UIRs) is proposed. First, a open-ended stub is tap-connected to a meandering UIR at its centre, and these two stub-loaded meandering UIRs are further placed at symmetrical locations with respect to a stub-loaded hairpin resonator. Secondly, by introducing two parallel coupled lines at the two sides of the stub-loaded hairpin resonator, a dual-band BPF with two passbands at 2.4 GHz and 5.2 GHz is constructed. Finally, a prototype filter is designed and fabricated, and its measured results are provided to verify the predicted dual-band filter design.

1. INTRODUCTION

With the development of modern wireless communication systems, the demand for dual-band microwave systems has increased rapidly. The systems require microwave bandpass filters (BPFs) to handle different frequency bands. So far, various techniques have been proposed to explore dual-band BPFs [1–8]. The simplest way to construct a dual-band filter is combining two different single-band filters [1, 2]. This approach is superior to others in terms of simple design and flexible passbands. However, the circuit usually occupies a large area, due to additional impedance-matching networks. The second method is to separate an entire wide passband into two relatively narrow passbands by cascading a wideband BPF with a narrowband bandstop filter [3, 4]. The third method is to construct two passbands by virtue of first two resonant frequencies of coupled stepped-impedance resonators (SIRs) [5]. In [6] and [7], a simple stub-loaded dual-mode resonator was employed for the dual-band filter design, but it is difficult to synthesize the corresponding dual-band coupling degrees. Another paper in [8] proposes a class of dual-band bandpass filters with SIRs and presents a rigorous synthesis method for these compact filters. An embedded dual-mode hairpin resonator is studied and used for a dual-band filter design [9]. In another method, multimode resonators (MMRs) have been attracting much attention of researchers with their advantage of compact size in the design of dual-passband filters on the microstrip-line MMRs [10] and slotted patches [11] or SIW MMR [12].

In this Letter, a novel dual-band BPF with a compact size is presented by coupling a stub-loaded hairpin resonator and two stub-loaded UIRs. The characteristics of these resonators are analyzed, and then applied to the dual-band BPF design. Finally, a prototype filter is designed and fabricated to provide experimental verification.

2. THEORETICAL ANALYSIS

As described in Figure 1(a), the conventional UIR is bent at both ends, and a stub is tap-connected in its centre. Compared with the existing stub-loaded resonators, the proposed one apparently has a

Received 21 October 2020, Accepted 28 December 2020, Scheduled 13 January 2021
* Corresponding author: Yun Xiu Wang (109wyx@163.com).
The authors are with the School of Electronic and Information Engineering, China West Normal University, Nanchong 637009, China.

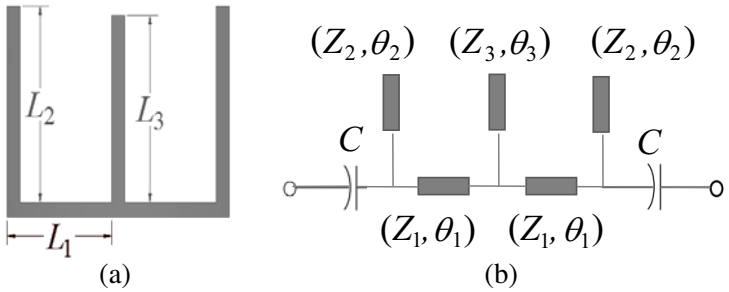

Figure 1. Layout of Stub-loaded meandering UIR and its transmission line models with loose coupling. (a) Layout. (b) Transmission line models.

miniaturized size. Its transmission line models is shown as in Figure 1(b). The resonator is loosely-coupled with I/O ports by $C = 0.01$ pF, here (Z_1, Z_2, and Z_3) denote characteristic impedances, and (θ_1, θ_2, and θ_3) indicate corresponding electrical lengths. The input admittance is given by

$$Y_{in} = jY\frac{\tan\theta_3 + 2\tan(\theta_1+\theta_2)}{1-[\tan\theta_3+\tan(\theta_1+\theta_2)]\cdot\tan(\theta_1+\theta_2)} \tag{1}$$

where $\theta_i = \beta L_i$, $Z_1 = Z_2 = Z_3 = 1/Y$. The resonant frequencies can be calculated by setting $Y_{in} = 0$, as follows:

$$\tan\theta_3 + 2\tan(\theta_1+\theta_2) = 0 \tag{2}$$

To investigate the resonant properties of a stub-loaded meandering UIR, its respective transmission line model shown in Figure 1(b) is analyzed in Agilent Advanced System (ADS) on a substrate with a thickness of 1.27 mm and dielectric constant of 10.8. Here, L_1=2.4 mm and $L_2 = L_3$=2.4 mm in Figure 1(a), and the corresponding electrical lengths and impedance for the stub-loaded resonator are chosen to be $\theta_1 = 25°$, $\theta_2 = \theta_3 = 40°$, and $Z_1 = Z_2 = Z_3 = 80\,\Omega$, in Figure 1(b). Based on the above analysis, the resonant property of the resonator is plotted in Figure 2. It can be seen that there is a transmission zero at 7.85 GHz between the second and third resonant modes due to the loaded stub, which can vastly improve the upper stopband with enhanced attenuation.

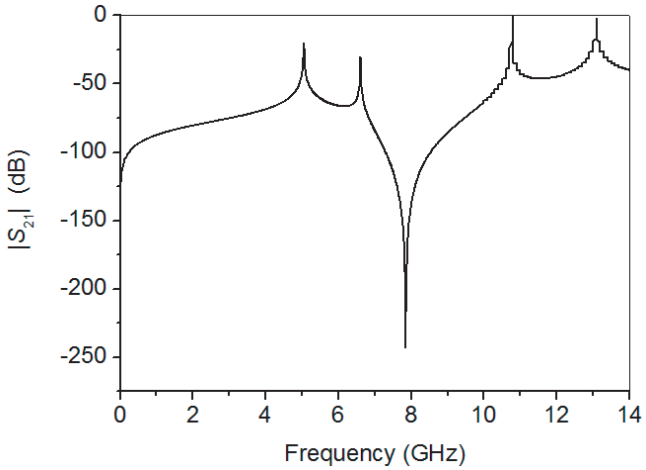

Figure 2. Frequency responses of the resonator circuits in Figure 1(b).

By appropriately folding a UIR at the centre, a coupled-line hairpin resonator with two stubs-loaded shown in Figure 3(a) can be constructed, here $L_4 = 5.6$ mm, $L_5 = L_6 = 5.4$ mm, $W_1 = 0.6$ mm, $W_2 = 0.3$ mm, $g = 0.2$ mm. Its transmission line model with loose coupling is shown in Figure 3(b), in which the corresponding electrical lengths and impedances are chosen to be $\theta_h = 42°$, $\theta_{ho} = \theta_{he} = 86°$,

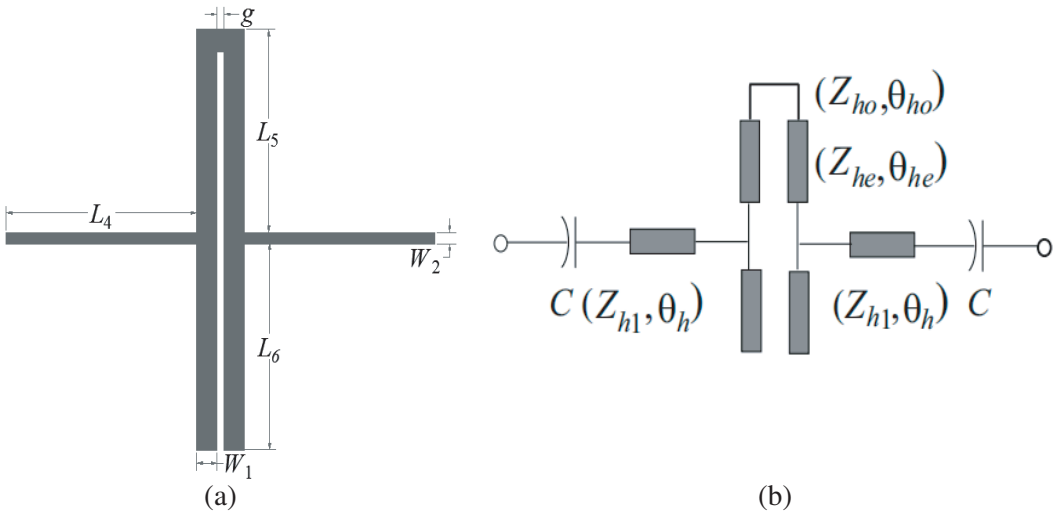

Figure 3. Layout of Stub-loaded hairpin resonator and its transmission line models with loose coupling. (a) Layout. (b) Transmission line models.

$Z_{h1} = 80\,\Omega$, $Z_{ho} = 35\,\Omega$, and $Z_{he} = 90\,\Omega$. As discussed in [13], it can generate transmission zeros between the first and second resonant modes under the condition of the impedance ratio $R = Z_{ho}/Z_{he} < 0.5$. In this letter, R is selected as 0.4, thereby achieving our desired two transmission zeros between the dual bands which ensure the good selectivity of the filter. The transmission zeros are calculated by

$$S_{21} = \frac{-jY_{h1}\Delta Y_1 \cot(\theta_{eff})}{Y_{h1}^2 \cot^2(\theta_{eff}) - \Delta Y_2 + jY_{h1}\cot(\theta_{eff})\Delta Y_1} = 0 \tag{3}$$

where

$$\begin{aligned} \Delta Y_1 &= 2Y_{he} + Y_{ho} - Y_{ho}\cot^2(\theta_{eff}) \\ \Delta Y_2 &= 2Y_{he}Y_{ho}\left(1 - \cot^2(\theta_{eff})\right) \\ Y_{ho} &= 1/Z_{ho;} \quad Y_{he} = 1/Z_{he;} \quad Y_{h1} = 1/Z_{h1} \end{aligned}$$

here θ_{eff} is the arithmetic-averaged electrical length of θ_{he} and θ_{ho} for the coupled-line section. Figure 4 plots the frequency responses of the hairpin resonator loosely-coupled with I/O ports by $C = 0.01$ pF. By properly adjust the lengths of coupled-line section and the stubs, the proposed resonator shows the emergence of two transmission zeros at 3.67 GHz and 4.8 GHz between the first and second resonant modes. This feature is because the two arms of the hairpin resonator are closely spaced, and there are both electric and magnetic couplings between them. Each arm of the hairpin resonator has the maximum electric field density at the end and the maximum fringe magnetic field density at both of the adjacent sides. As described in [14], this will result in producing transmission zeros by appropriately tuning the parameters of electric coupling and magnetic coupling, and the coupling mechanism of transmission zero generation is investigated in detail in [14].

3. FILTER DESIGN AND IMPLEMENTATION

In view of above characteristics, a Chebyshev BPF using a stub-loaded hairpin resonator and two stub-loaded meandering UIRs coupled is designed with central frequencies, $f_0^{\mathrm{I}} = 2.4$ GHz and f_0^{II}=5.2 GHz. Its coupling topology structure is shown as in Figure 5. The passband bandwidths of this filter depend on the external quality factors and coupling coefficients. Therefore, considering the layout of the I/O structure of Figure 6(a), the gap g_1 and coupling length L determine the external quality factors. The gap g and s, shown as in Figure 6(b) have relationship with the coupling coefficients. In addition, because two arms of each hairpin resonator are closely spaced, they function as a pair of coupled line themselves, which can have an effect on the coupling as well. According to the coupling coefficients,

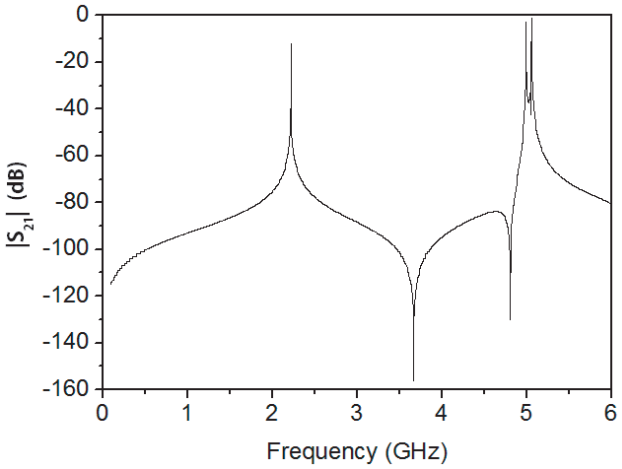

Figure 4. Frequency responses of the resonator circuits in Figure 3(b).

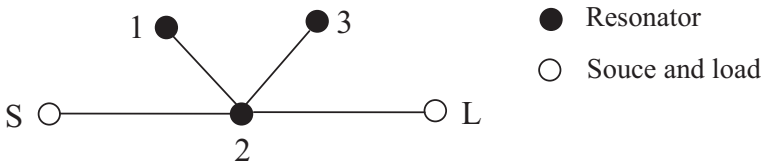

Figure 5. The coupling topology structure of the BPF.

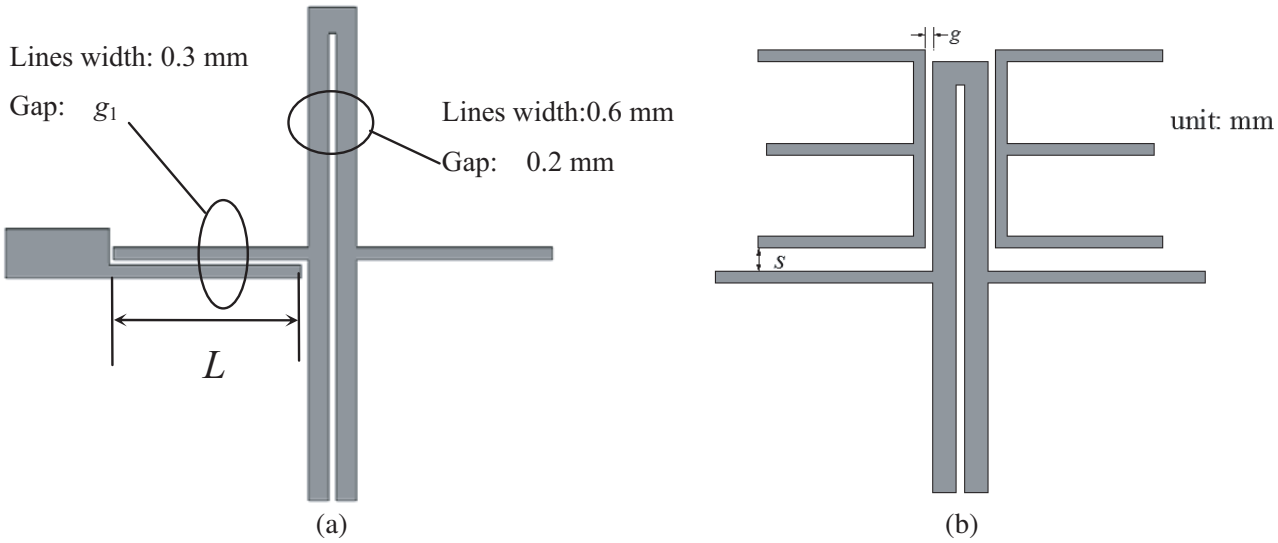

Figure 6. (a) Layout of I/O structure. (b) Coupling aperture between two adjacent resonators.

we can only roughly give the spacing between resonators. Therefore, to design this type of filter more accurately, a design approach employing full-wave simulation is applied to optimize it.

In order to demonstrate the performance of the proposed filter, the filter circuit is synthesized and optimally designed, and its relevant layout with detailed dimensions is depicted in Figure 7(a). Figure 7(b) describes the simulated and measured results. It can be observed that the stopband is now expanded up to 12.7 GHz with insertion loss larger than 17 dB, where the maximum in-band return losses are 32 dB and 19 dB; the minimum insertion losses are 1.37 dB and 1.23 dB at the 2.34 GHz and the 5.18 GHz; the measured 3-dB fractional bandwidths are about 10.5% and 5.5% at 2.34 GHz

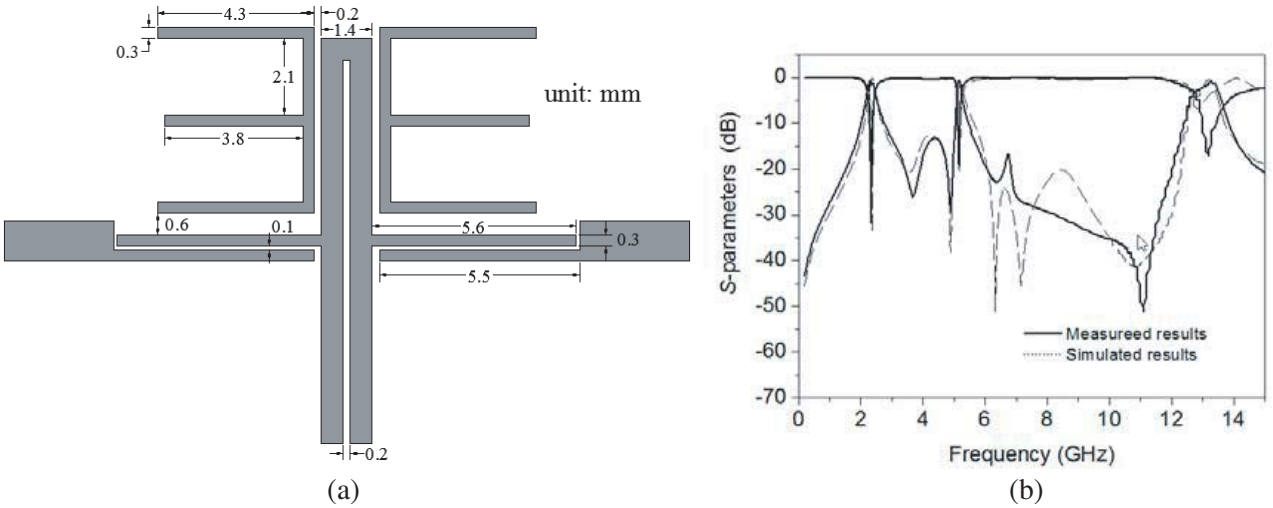

Figure 7. Optimally designed filter. (a) Dimensional layout. (b) Simulated and measure results.

Figure 8. Photograph of the fabricated bandpass filter.

and 5.18 GHz. Simulated results almost agree with measured ones over a wide frequency. The slight discrepancy of simulated and measured results is mainly caused by unexpected tolerance in fabrication and the added input/output subminiature A (SMA) connectors. From the frequency responses of the stub-loaded meandering UIR and stub-loaded hairpin resonator, shown as in Figure 2 and Figure 4, it can be seen that the first resonant modes of stub-loaded hairpin resonator form the first passband, and the first resonant modes of stub-loaded meandering UIR compose the second passband. Figure 8 shows a photograph of the fabricated bandpass filter. Finally, the comparisons of the proposed BPF with other typical dual-band BPFs are summarized in Table 1. It clearly shows that the bandpass filter designed in this study has the advantages of compact size and good out-of-band rejection to those reported in [15–18]. λ_g is the guided wavelength at the first central frequency 2.4 GHz. Moreover, the design method and structure are simple, which is suitable for engineering application.

Table 1. Comparison with other reported bandpass filters.

References	Central frequencies (GHz)	FBW(%)	Stop-band (GHz)	Size $\lambda_g \times \lambda_g$
[15]	2.42/5.24	7.4/9.2	7 ($2.9f_0^{\mathrm{I}}$)	0.48×0.45
[16]	2.4/3.5	8.3/5.1	5.5 ($2.3f_0^{\mathrm{I}}$)	0.93×0.26
[17]	2.4/5.16	13.7/6.3	/	0.46×0.46
[18]	2.4/5	14.6/5.8	9.2 ($3.8f_0^{\mathrm{I}}$)	0.58×0.26
This work	**2.4/5.2**	**10.5/5.5**	**12.7 ($5.3f_0^{\mathrm{I}}$)**	0.30×0.33

4. CONCLUSION

In this letter, a simple and effective design method for a dual-band filter has been presented with high frequency selectivity. After detailed optimal design, a prototype has been implemented following the given design procedure. The experimental results display that the proposed filter exhibits good operation performance.

ACKNOWLEDGMENT

This work is supported in part by the Meritocracy Research Funds of China West Normal University under Grant 17YC054, Key projects of Sichuan Education Department under Grant 16ZA0172, and Study Abroad and Return Fund of China West Normal University under Grant 15B001.

REFERENCES

1. Miyake, H., S. Kitazawa, T. Ishizaki, T. Yamada, and Y. Nagatomi, "A miniaturized monolithic dual band filter using ceramic lamination technique for dual mode portable telephones," *IEEE MTT-S Int. Microw. Symp. Dig.*, Vol. 2, 789–792, 1997.
2. Chen, C. Y. and C. Y. Hsu, "A simple and effective method for microstrip dual-band filters design," *IEEE Microw. Wirel. Compon. Lett.*, Vol. 16, No. 5, 246–248, 2006.
3. Tsai, L. C. and C. W. Hsue, "Dual-band bandpass filters using equal length coupled-serial-shunted lines and Z-transform technique," *IEEE Trans. Microw. Theory Techn.*, Vol. 52, No. 4, 1111–1117, 2004.
4. Chen, D., L. Zhu, and C. Cheng, "A novel dual-band bandpass filter with closely spaced passbands," *IEEE Microw. Wireless Compon. Lett.*, Vol. 24, No. 1, 38–40, 2014.
5. Ren, B. P., Z. Wang, H. W. Liu, A. Gu, et al., "Miniature dual-band bandpass filter using modified quarter-wavelength SIRs with controllable passbands," *Electron. Lett.*, Vol. 55, No. 1, 38–40, 2019.
6. Zhang, X. Y., J. X. Chen, Q. Xue, and S. M. Li, "Dual-band bandpass filters using stub-loaded resonators," *IEEE, Microw. Wireless Compon. Lett.*, Vol. 17, No. 8, 583–585, 2007.
7. Mondal, P. and M. K. Mandal, "Design of dual-band bandpass filters using stub-loaded open-loop resonators," *IEEE Trans. Microw. Theory Techn.*, Vol. 56, No. 1, 150–155, 2008.
8. Zhang, S. B. and L. Zhu, "Synthesis design of dual-Band bandpass filters with stepped-impedance resonators," *IEEE Trans. Microw. Theory Techn.*, Vol. 61, No. 5, 1812–1819, 2013.
9. Ma, P. Y., B. Wei, J. S. Hong, et al., "Coupling matrix compression technique for high-isolation dual-mode dual-band filters," *IEEE Trans. Microw. Theory Techn.*, Vol. 66, No. 6, 1–8, 2018.
10. Zhang, J. L., M. He, H. H. Chen, et al., "Bandpass filters using multi-mode square ring resonators," *IET Microwaves, Antennas & Propagation*, Vol. 12, No. 10, 1656–1665, 2018.
11. Chen, J. X., C. Shao, J. Shi, and Z.-H. Bao, "Multilayer independently controllable dual-band bandpass filter using dual-mode slotted-patch resonator," *Electron. Lett.*, Vol. 49, No. 9, 605–607, 2013.
12. Zhang, H., W. Kang, and W. Wu, "Miniaturized dual-band SIW filters using E-shaped slotlines with controllable center frequencies," *IEEE Microw. Wireless Compon. Lett.*, Vol. 28, No. 4, 311–313, 2018.
13. Luo, S., L. Zhu, and S. Sun, "Stopband-expanded low-pass filters using microstrip coupled-line hairpin units," *IEEE Microw. Wirel. Compon. Lett.*, Vol. 18, No. 8, 506–508, 2008.
14. Chu, Q. X. and H. Wang, "A compact open-loop filter with mixed electric and magnetic coupling," *IEEE Trans. Microw. Theory Techn.*, Vol. 56, No. 2, 431–439, 2008.
15. Deng, K., S. J. Sun, S. Yang, B. Wu, and C. H. Liang, "Two kinds of dualband bandpass filter based on a single square ring resonator," *Progress In Electromagnetics Research C*, Vol. 44, 251–261, 2013.
16. Chen, F. C. and Q. X. Chu, "Novel multistub loaded resonator and its application to high-order dual-band filters," *IEEE Trans. Microwave Theor. Tech.*, Vol. 58, No. 6, 1551–1556, 2010.

17. Li, Y. C., H. Wong, and Q. Xue, "Dual-mode dual-band bandpass filter based on a stub-loaded patch resonator," *IEEE Microw. Wirel. Compon. Lett.*, Vol. 21, No. 10, 525–527, 2011.
18. Shi, F. L., L. Zhao, and X.-L. Zhang, "Dual-band filter with high selectivity and wide stopband rejection," *Int. J. RF Microw. Comput.-Aided. Eng.*, Vol. 30, No. 11, 2020.